KI REPORTS
KIReports.org
CLINICAL RESEARCH

The Role of Glomerular Epithelial Injury in Kidney Function Decline in Patients With Diabetic Kidney Disease in the TRIDENT Cohort

Matthew B. Palmer[1], Amin Abedini[2,3], Casey Jackson[2,3], Shira Blady[2], Shatakshee Chatterjee[2,3], Katie Marie Sullivan[2,3], Raymond R. Townsend[3], Jens Brodbeck[4], Salem Almaani[5], Anand Srivastava[6], Rupali Avasare[7], Michael J. Ross[8], Amy K. Mottl[9], Christos Argyropoulos[10], Jonathan Hogan[2] and Katalin Susztak[2,3]

[1]Department of Pathology and Laboratory Medicine, University of Pennsylvania, Perelman School of Medicine, Philadelphia, Pennsylvania, USA; [2]Renal, Electrolyte, and Hypertension Division, Department of Medicine, University of Pennsylvania, Perelman School of Medicine, Philadelphia, Pennsylvania, USA; [3]Institute of Diabetes, Obesity, and Metabolism, University of Pennsylvania, Perelman School of Medicine, Philadelphia, Pennsylvania, USA; [4]Inflammation & Respiratory Therapeutics, Gilead Sciences Inc., Foster City, California, United States; [5]Division of Nephrology, The Ohio State University Wexner Medical Center, Columbus, Ohio, USA; [6]Division of Nephrology and Hypertension, Center for Translational Metabolism and Health, Institute for Public Health and Medicine, Northwestern University Feinberg School of Medicine, Chicago, Illinois, USA; [7]Department of Medicine, Nephrology, Oregon Health & Science University, Portland, Oregon, USA; [8]Division of Nephrology, Albert Einstein College of Medicine/Montefiore Medical Center, Bronx, New York, USA; [9]University of North Carolina Kidney Center, University of North Carolina at Chapel Hill, Chapel Hill, North Carolina, USA; and [10]Department of Internal Medicine, Division of Nephrology, University of New Mexico Health Sciences Center, Albuquerque, New Mexico, USA

Introduction: Although diabetic kidney disease (DKD) is responsible for more than half of all chronic and end-stage kidney disease (ESKD), the association of light (LM) and electron microscopic (EM) structural changes with clinical parameters and prognosis in DKD is incompletely understood.

Methods: This is an interim analysis of 62 patients diagnosed with biopsy-confirmed DKD from the multicenter TRIDENT (Transformative Research in Diabetic Nephropathy) study. Twelve LM and 8 EM descriptors, representing changes in glomeruli, tubulointerstitium, and vasculature were analyzed for their relationship with clinical measures of renal function. Patients were followed every 6 months.

Results: Multivariable linear regression analysis revealed that estimated glomerular filtration rate (eGFR) upon enrollment correlated the best with interstitial fibrosis. On the other hand, the rate of kidney function decline (eGFR slope) correlated the most with glomerular lesions including global glomerulosclerosis and mesangiolysis. Unbiased clustering analysis based on histopathologic data identified 3 subgroups. The first cluster, encompassing subjects with the mildest histologic lesions, had the most preserved kidney function. The second and third clusters had similar degrees of kidney dysfunction and structural damage, but differed in the degree of glomerular epithelial cell and podocyte injury (podocytopathy DKD subtype). Cox proportional hazard analysis showed that subjects in cluster 2 had the highest risk to reach ESKD (hazard ratio: 17.89; 95% confidence interval: 2.13–149.79). Glomerular epithelial hyperplasia and interstitial fibrosis were significant predictors of ESKD in the multivariate model.

Conclusion: The study highlights the association between fibrosis and kidney function and identifies the role of glomerular epithelial changes and kidney function decline.

Kidney Int Rep (2021) **6,** 1066–1080; https://doi.org/10.1016/j.ekir.2021.01.025
KEYWORDS: diabetic kidney disease; end-stage kidney disease; glomerular epithelial injury; kidney function; pathological descriptors

Correspondence: Katalin Susztak, University of Pennsylvania, Perelman School of Medicine, 3400 Civic Center Boulevard, Smilow Translational Building 12–123, Philadelphia, Pennsylvania 19104, USA. E-mail: ksusztak@pennmedicine.upenn.edu

MBP and AA contributed equally.

Received 1 November 2020; revised 11 January 2021; accepted 18 January 2021; published online 3 February 2021

Diabetes mellitus (DM) still shortens life expectancy by approximately 10 years.[1] Although improvements in glycemic and blood pressure control have brought reductions in many of the complications of diabetes, including 70% decline in cardiovascular disease and amputations,[2] the incidence of ESKD rates

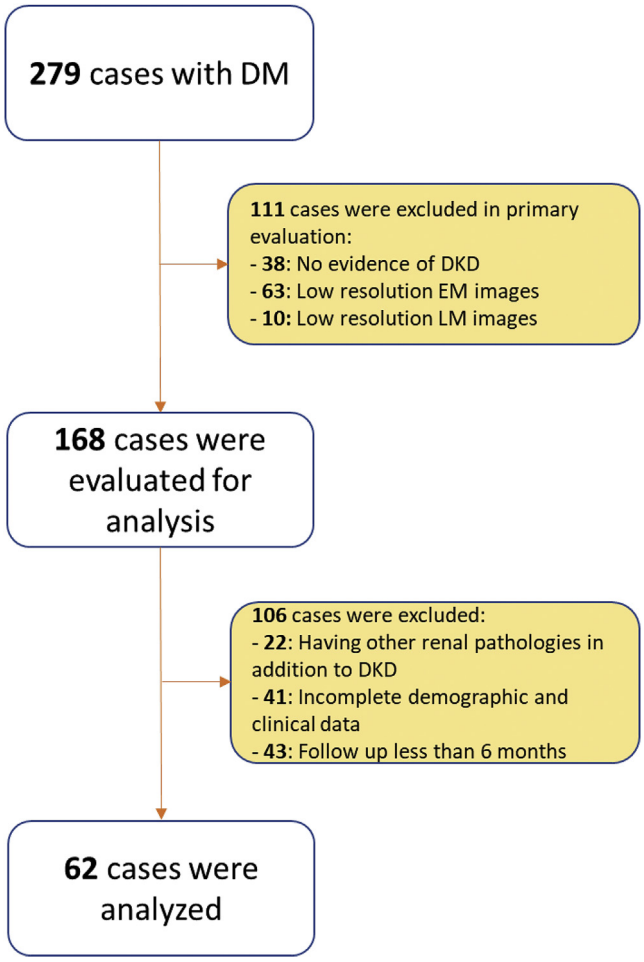

Figure 1. Patients' selection for the analysis. DKD, diabetic kidney disease; DM, diabetes mellitus; EM, electron microscopy; LM, light microscopy.

has only minimally changed over the past 20 years.[3] The excess mortality in DM is linked and strongly correlates with the presence of kidney disease.[3]

The pathogenesis of DKD is still poorly understood. There is a lack of robust animal model systems that fully recapitulate the glomerulosclerosis, tubulointerstitial fibrosis, and decline in kidney function that are hallmarks of human DKD.[4] Genetic studies have only been minimally successful in identifying variants associated with DKD.[5] A recent study analyzing subjects with type 1 diabetes highlighted variants in collagen IV and other podocyte genes, potentially implicating an important pathogenic role for podocytes.[6]

DKD is clinically defined by the presence of albuminuria and a decline in kidney function.[7] Although albuminuria is a classic clinical diagnostic criterion for DKD, more recent data demonstrated that 40% to 50% of patients with DM develop decreased eGFR in the absence of albuminuria,[8–11] indicating that the clinical course of DKD might have evolved over the decades since the original description by Mogensen *et al.*[12]

Histologic analysis demonstrating the presence of glomerular basement membrane (GBM) thickening with or without mesangial expansion remains the diagnostic gold standard for DKD,[13] and provide the basis for the Renal Pathology Society (RPS) classification system for diabetic nephropathy.[13] The RPS classification was the first unified system for staging DKD severity.[13] The simplicity and reproducibility of the RPS system are its strengths; however, it is incomplete in not capturing tubulointerstitial and vascular changes, which are likely important in DKD progression.[14] For example, tubulointerstitial fibrosis is observed in all chronic progressive kidney disease and shows a strong association with kidney function.[15–18]

One of the most significant clinical issues is that patients with DKD show very significant heterogeneity in their rate of kidney function decline. The chronic renal insufficiency cohort study indicates that the mean eGFR decline in patients with diabetes and already stage 3 to 4 chronic kidney disease (CKD) is approximately 2 ml/min per year,[15] but some patients present with very rapid kidney function decline. Despite extensive efforts to identify reliable biomarkers for kidney function decline, there are still only a limited number of prognostic biomarkers. Elevated blood pressure and smoking has reproducibly been associated with worse prognosis regardless of disease etiology.[19] Baseline kidney function (eGFR) is one of the strongest determinants of kidney function change overall.[20] Patients with elevated serum level of tumor necrosis factor receptor 1 and tumor necrosis factor receptor 2 have an increased incidence of reaching ESKD.[21] Most clinical trials continue to enroll subjects with large amounts of proteinuria, as these subjects seem to be enriched for rapid kidney function decline as an outcome approved by the Food and Drug Administration.[22] Albuminuria, however, shows very significant variability and its relationship with renal outcomes has not been systematically evaluated, thus the Food and Drug Administration does not accept change in albuminuria as a valid outcome for drug registration.[23]

Given the lack of good clinical and noninvasive biomarkers for kidney function decline, several studies have analyzed whether histologic changes can provide predictors of outcome. Some recent reports highlighted a correlation between kidney fibrosis and kidney function decline[16–18,24]; however, these results were not adjusted for baseline covariates such as eGFR, included patients with heterogenous histopathologic diagnoses, or were from a single center. Some of the most detailed kidney structure studies have been performed on the ethnically distinct Pima Indian population with early diabetic kidney disease.[25–27] These studies highlighted changes in GBM and podocytes and

Table 1. Light and electron microscopy parameters and descriptors used in the study

Descriptors	Definitions
KW nodules (No/Yes)	Round mesangial sclerosing lesions with hypocellular center[13]
RPS DN class (1/2/3/4)	RPS classification of diabetic nephropathy[13]
Segmental sclerosis (0/1/2/3/4)	Segmental solidification of the glomerular tuft, scored as % quartiles[57]
Global sclerosis (0/1/2/3/4)	Solidification of 100% of the glomerular tuft, scored as % quartiles[57]
Glomerular epithelial hypertrophy (0/1/2/3)	Enlarged epithelial nuclei and/or cytoplasm[57]; unifocal (1), multifocal (2), diffuse (3)
Glomerular epithelial hyperplasia (0/1/2/3)	≥2 layers of epithelial cells overlying the GBM[57]; unifocal (1), multifocal (2), diffuse (3)
Mesangiolysis (No/Yes)	Dissolution of mesangial matrix ± microaneurysms
Insudative lesion (No/Yes)	Hyaline eosinophilic material deposition within the tuft or in Bowman's capsule[58]
Interstitial fibrosis	Interstitium expanded by collagenous extracellular matrix, scored as % area of sampled cortex
Interstitial lymphocyte (0/1/2/3)	Presence of interstitial lymphocytes; unifocal (1), multifocal (2), diffuse (3)
Arteriolar hyalinosis (0/1/2/3)	Hyaline eosinophilic material deposition within arteriolar wall; unifocal (1), multifocal (2), diffuse (3)
Intimal fibrosis (0/1/2/3)	Expansion of vascular wall intima by collagenous material; <50% thickness of media (1), 50%–100% thickness of media (2), >100% thickness of media (3)
Avg GBM thickness (nm)	Mean of EM measurements taken where grid line intersects endothelium and GBM, excluding areas with segmental collapse or solidification[32]
GBM Lamina densa remodeling (0/1/2/3)	Lamina densa with lamellation, fraying or lucent patches on EM; focal (1), multifocal (2), diffuse (3)
GBM duplication (0/1/2/3)	Deposition of an inner layer of basement membrane-like material on EM; focal (1), multifocal (2), diffuse (3)
FPW (μm)	Mean distance between adjacent podocyte filtration slits on filtering capillary walls[31]
Foot process effacement	Loss of podocyte foot processes, excluding areas where 2 GBMs touch, scored as %[42]
Endothelial fenestration loss (0/1/2/3)	Loss of endothelial pores resulting in solid rim of cytoplasm[42] focal (1), multifocal (2), diffuse (3)
Mesangial hyaline (0/1/2/3)	Deposition of fine, uniform, electron-dense material lacking sharp edges[42]; focal (1), multifocal (2), diffuse (3)
Mesangial matrix increase (0/1/2/3)	Expansion of mesangial matrix beyond width of 2 mesangial nuclei; mild (1), moderate (2), severe (3)

Avg GBM, average glomerular basement membrane; FPW, foot process width; KW, Kimmelstiel-Wilson Nodule; RPS DN class, Renal Pathology Society diabetic nephropathy class.

their correlation with albuminuria.[26,27] The role of these changes and their association with clinically meaningful kidney function decline, such as reaching CKD or ESKD remains unclear.

TRIDENT is a multicenter observational cohort aimed to identify changes associated with kidney function decline in patients with DM in an unbiased manner via multi-omics characterization of kidney tissue specimens.[28] In the present study, we analyzed histopathologic features obtained from a comprehensive descriptor-based scoring system, including LM and EM, in a subset of TRIDENT patients to explore the relationship between histopathologic changes, clinical parameters, and outcomes.

METHODS

Study Population

The study protocol was approved by the institutional review board of the University of Pennsylvania. Informed consent was obtained from all participants.

This is an interim analysis of the TRIDENT cohort study and includes participants enrolled as of January 2018. Details of the study design have been previously published.[28] In brief, patients with a clinical diagnosis of type I or type II DM undergoing clinically indicated kidney biopsy were consented for the study. Only participants with central pathology reading consistent with RPS diagnostic criteria for diabetic glomerulosclerosis were followed longitudinally.

Detailed clinical and demographic parameters were recorded on enrollment. Kidney biopsy materials, including digitally scanned whole slide images and digital electron microscopy images, were collected and stored in a centralized database. Subjects were followed every 6 months and changes in clinical parameters were recorded in the database.

For this analysis, exclusion criteria included the following: (i) poor quality LM or EM images, (ii) the presence of superimposed nondiabetic glomerular pathologies (amyloidosis, cryoglobulinemic glomerulonephritis, membranous glomerulopathy, IgA nephropathy, minimal change disease, and focal segmental glomerulosclerosis), (iii) incomplete demographic or clinical data, (iv) patients with uncontrolled hypertension, and (v) cases with less than 6 months of follow-up. Figure 1 shows the patients' selection for the study. This interim analysis comprises 62 cases of 279 cases collected from 11 clinical centers.

Clinical and Laboratory Data Collection

Demographic data was retrieved from the TRIDENT study database. The values at time of biopsy were considered as baseline and the latest values were considered as follow-up time. eGFR was calculated using the Chronic Kidney Disease Epidemiology Collaboration equation.[29] Prior reports indicated that kidney function decline mostly follows a linear pattern at late stages of kidney disease, which we also confirmed in our study participants.[30] eGFR change

Table 2. Baseline clinical characteristics of the participants in the cohort

Variables	Value
Gender, male/female, *n* (%)	42(67.7)/20(32.3)
Age (yr)	53.4 ± 12.49
Race, *n* (%)	
White	38 (61.3)
African American	19 (30.6)
Asian	4 (6.5)
American Indian	1 (1.6)
Type of DM, I/II, *n* (%)	6(9.7)/56(90.3)
Duration of DM (yr)	15.68 ± 11.14
Smoking, *n* (%)	12 (19.4)
Family history of CKD, *n* (%)	10 (16.1)
BMI (kg/m^2)	34.05 ± 7.53
SBP (mm Hg)	140.94 ± 22.17
DBP (mm Hg)	76.61 ± 12.48
eGFR (ml/min per 1.73 m^2)	32.79 ± 16.88
UPCR (mg/g), median (IQR)	4,640 (7,250)
HbA1C, *n* (%)	7.87 ± 1.81
Biopsy indications, *n* (%)	
Unusual degree of proteinuria	38 (61.3)
Unusual urinary findings	9 (14.5)
Rapid loss of renal function	13 (21)
Suspicion of non-DKD	2 (3.2)
Medication history, *n* (%)	
Insulin	39 (62.9)
Oral hypoglycemic agents	35 (56.4)
Statins	46 (74.2)
ACEi	21 (33.9)
ARB	17 (27.4)
B-blockers	29 (46.8)
Calcium channel blockers	33 (53.2)

ACEi, angiotensin converting enzyme inhibitors; ARB, angiotensin II receptor blockers; BMI, body mass index; CKD, chronic kidney disease; DBP, diastolic blood pressure; DM, diabetes mellitus; eGFR, estimated glomerular filtration rate; HbA1C, hemoglobin A1C; IQR, interquartile range; SBP, systolic blood pressure; UPCR, urine protein to creatinine ratio.

percentage was calculated with the following equation: $\frac{eGFR\ (Follow\ Up) - eGFR\ (Baseline)}{eGFR\ (Baseline)} \times 100$. The values obtained from this equation were adjusted for follow-up time and normalized to 1 year. Urine protein to creatinine ratio (UPCR) was measured in the random spot urine specimens. Fold change of UPCR was measured by dividing the UPCR-Follow Up value with baseline UPCR measurement, then this ratio was adjusted for the follow-up time by normalizing to 1 year. Serum creatinine and UPCR were processed in local laboratories.

LM and EM Descriptor Measurements

Twelve LM and 8 EM parameters associated with diabetic nephropathy and general renal pathology were scored and are defined in Table 1. Scoring was performed by a single renal pathologist in an unbiased manner, blinded to the demographic and clinical data. Scoring was based on the evaluation of all whole slide imaging available for each case and included hematoxylin-eosin, periodic acid-Schiff, trichrome, and silver-stained sections. The mean numbers of LM and EM images assessed for each patient were 6 and 30, respectively. Podocyte foot process width was measured and calculated as previously described.[31] GBM thickness was calculated as the mean of measurements taken at the intersection of grid lines with endothelium on filtering capillary wall segments.[32]

Table 3. Feature of the patients at last follow-up visit

Variables	Value
Follow-up time (mo)	10.55 ± 5.05
BMI (kg/m^2)	33.87 ± 8.43
SBP (mm Hg)	137.16 ± 20.08
DBP (mm Hg)	75.05 ± 11.77
eGFR (ml/min per 1.73 m^2)	24.98 ± 15.55
eGFR change (%), median (IQR)	-18.26 (45)
eGFR change (%/y), median (IQR)	-25.84 (58)
UPCR (mg/g), median (IQR)	5010 (8260)
UPCR fold change, median (IQR)	0.94 (1.31)
UPCR fold change (/y), median (IQR)	1.29 (2.15)
ESKD progression, *n* (%)	17 (27.4)

BMI, body mass index; DBP, diastolic blood pressure; eGFR, estimated glomerular filtration rate; ESKD, end-stage kidney disease; IQR, interquartile range; SBP, systolic blood pressure; UPCR, urine protein to creatinine ratio.

Statistical Analysis

Continuous data were presented as mean ± SD and median (interquartile range [IQR]). Associations between variables were assessed using Spearman rank correlation. Stepwise, multiple linear regression was used to determine independent predictors of eGFR and UPCR at baseline and their changes. Baseline UPCR and UPCR fold change and eGFR percentage change were non-normally distributed and were log transformed.

To identify unbiased subgroups based on LM and EM descriptors, unsupervised hierarchical clustering was performed on the scaled data using the Ward's method with Euclidean distances.[33] The optimal number of clusters was determined by average silhouette method.[34] Data are presented as cluster dendrograms. Differences between clusters, in terms of LM, EM, and clinical parameters, were visualized on radar plots. To compare the continuous and categorical clinical, laboratory, and pathological parameters between groups, 1-way analysis of variance and χ^2 tests were used, respectively.

To compare the probability of reaching ESKD in the different subgroups of the patients based on the pathological descriptors, Kaplan-Meier life table survival analysis was performed. Reaching ESKD and initiation of renal replacement therapy was considered as outcome in the survival analysis. The time from the renal biopsy to the initiation of the renal replacement therapy was recorded and included in the analysis. Log-rank test was performed to compare the survival probability in different subgroups. Cox proportional

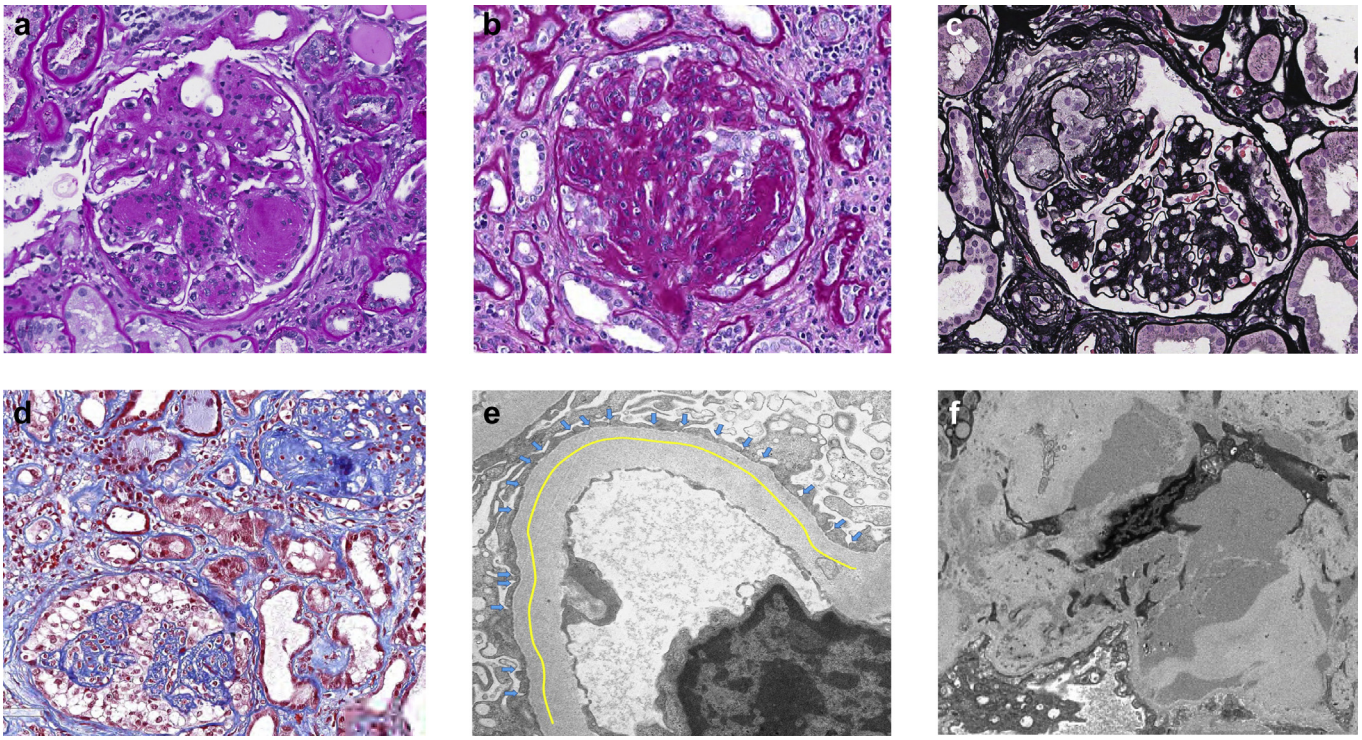

Figure 2. Illustrations of some LM and EM lesions scored in the study. (a) Kimmelstiel-Wilson nodules defined as nodular mesangial sclerosis with hypocellular center (periodic acid-Schiff [PAS], original magnification ×400). (b) Glomerular epithelial hypertrophy and hyperplasia with enlarged epithelial cells forming at least 2 layers (PAS, original magnification ×400). These podocyte changes may be present in the form of podocytopathic lesions such as (c) tip lesions or (d) collapsing lesions (Jones silver, original magnification ×400, and trichrome, original magnification ×200, respectively). (e) Mean foot process width was measured by dividing the length of a segment of filtering capillary wall (yellow line) by the number of podocyte filtration slits (blue arrows) (electron micrograph, original magnification ×12,000). (f) Mesangial hyaline defined as deposits of fine, uniform, moderately electron-dense material lacking sharp edges (electron micrograph, original magnification ×6000). EM, electron microscopy; LM, light microscopy.

hazard ratio analysis was applied to estimate the hazard ratio of ESKD progression on different groups of patients in univariate and multivariate manners. Analyses were performed using RStudio (v3.6.2) (R Development Core Team, Vienna, Austria) and SPSS (v26.0) (SPSS Inc; Chicago, IL). GraphPad Prism (v8.3.0) (GraphPad Software LLC, La Jolla, CA) was used to draw heat maps.

RESULTS

Cohort characteristics

The baseline characteristics of the study subjects are shown in Table 2. Sixty-two patients from the TRIDENT cohort were included in the current interim analysis; 42 patients (67.7 %) were men and the median age was 52.5 (IQR: 18) years. Nineteen participants (30.6%) were African American. On enrollment, 45% of patients had hypertension (defined as blood pressure $>$ 140/90) and 93.5% of patients took antihypertensive medications. The glycemic control was suboptimal (HbA1C $\geq$ 8 %) in 32 subjects (51.6%). At study initiation, 54.8 % had eGFR $<$ 30 ml/min per 1.73 m^2 and none of the patients were on dialysis at the time of biopsy or received renal transplantation. More than half (59.7%) of the analyzed subjects had nephrotic range proteinuria (UPCR $>$ 3500 mg/g). Overall, the subgroup included a diverse study population with variable clinical parameters.

Table 3 shows the clinical characteristics of patients at their most recent follow-up visit. Patients were followed for 10.6 (SD 5) months after the kidney biopsy. The UPCR values did not show a statistically significant difference between enrollment and the last follow-up visit ($P = 0.12$). At their last visits, 69.4% of patients had eGFR $<$ 30 ml/min per 1.73 m^2 and 21 patients (33.9%) had eGFR decline $>$ 40%. The median eGFR decline was −7.49 (IQR 15.77) ml/min per 1.73 m^2 per year. Overall, 17 patients (27.4 %) progressed to ESKD. There was a significant difference in eGFR between enrollment and last follow-up visit ($P = 0.0001$) indicating disease progression.

Histopathologic Changes in the TRIDENT Cohort

Histopathologic changes were evaluated by applying a descriptor-based scoring system to include parameters associated with diabetic nephropathy and other renal pathologies involving glomeruli, tubulointerstitium,

Table 4. Light microscopic findings in participants

Variables	Values
KW nodules (No/Yes), *n* (%)	16 (25.8)/46 (74.2)
RPS DN class (1/2/3/4), *n* (%)	2 (3.2)/ 12 (19.4)/ 35 (56.5)/ 13 (21)
Segmental sclerosis (0/1/2/3/4), *n* (%)	29 (46.8)/ 29 (46.8)/ 2 (3.2)/ 2 (3.2)/0
Global sclerosis (0/1/2/3/4), *n* (%)	2 (3.2)/22 (35.5)/ 23 (37.1)/ 8 (12.9)/ 7 (11.3)
Glomerular epithelial hypertrophy (0/1/2/3)	47 (75.8)/ 15 (24.2)/0/0
Glomerular epithelial hyperplasia (0/1/2/3)	51 (82.3)/ 11 (17.7)/0/0
Mesangiolysis (No/Yes), *n* (%)	40 (64.5)/ 22 (35.5)
Insudative lesion (No/Yes), *n* (%)	37 (59.7)/ 25 (40.3)
Interstitial fibrosis (0–25%/25–50%/50–75%/ 75–100%), *n* (%)	11 (17.7)/19 (30.6)/17 (27.4)/ 15 (24.2)
Interstitial lymphocyte (0/1/2/3), *n* (%)	2 (3.2)/16 (25.8)/39 (62.9)/5 (8.1)
Arteriolar hyalinosis (0/1/2/3), *n* (%)	11 (17.7)/27 (43.5)/16 (25.8)/ 8 (12.9)
Intimal fibrosis (0/1/2/3), *n* (%)	0/20 (32.3)/27 (43.5)/15 (24.2)

KW, Kimmelstiel-Wilson nodule; RPS DN class, Renal Pathology Society diabetic nephropathy class.

Table 5. Electron microscopic findings in participants

Variables	Values
Avg GBM thickness (nm)	778.87 ± 198.33
GBM Lamina Densa remodeling (0/1/2/3), *n* (%)	27 (43.5)/24 (38.7)/2 (3.2)/ 9 (14.5)
GBM Duplication (0/1/2/3), *n* (%)	37 (59.7)/ 15 (24.2)/ 10 (16.1)/0
Avg FPW (μm)	1.87 ± 0.89
Foot process effacement (0–25%/25%–50%/50%–75%/75%–100%), *n* (%)	5 (8.1)/14 (22.6)/29 (46.8)/ 14 (22.6)
Endothelial fenestration loss (0/1/2/3), *n* (%)	6 (9.7)/ 35 (56.5)/ 17 (27.4)/ 4 (6.5)
Mesangial hyaline (0/1/2/3), *n* (%)	23 (37.1)/19 (30.6)/ 10 (16.1)/10 (16.1)
Mesangial matrix increase (0/1/2/3), *n* (%)	0/4 (6.5)/11 (17.7)/ 47 (75.8)

Avg FPW, average foot process width; Avg GBM, average glomerular basement membrane.

and vessels. Figure 2 illustrates images of some LM and EM descriptors used. Tables 4 and 5 show the results of LM and EM scoring for the cohort, respectively. Most patients (77.5 %) were classified as RPS class III or IV. Approximately 24% of patients had greater than 50% global glomerulosclerosis, and segmental sclerosis was present in most (53.2%). Glomerular epithelial cell hypertrophy and hyperplasia were seen in 24.2% and 17.7% of participants, respectively. Thirty-two (51.6%) patients had interstitial fibrosis greater than 50%. A common and expected vascular finding was arteriolar hyalinosis; seen in 82.2% of the cases.

EM scoring confirmed the expected marked increase in GBM thickness, with a median of 763 (IQR 244) nm. Podocyte injury was a prominent but variable finding on EM, measured in part as increased mean foot process width (1.71 [IQR 1.12] μm). Greater than 50% podocyte foot process effacement was seen in 69.4% of patients. All cases showed mesangial matrix increase on EM, and mesangial hyaline deposits were present in 62.8%.

Interstitial Fibrosis Was an Independent Predictor of eGFR on Enrollment, But Glomerular Pathologies Predicted eGFR Change

Next, we examined the relationship among clinical, demographic, and structural (EM and LM) parameters. The Spearman ranked correlation values are presented in Figure 3 and Supplementary Table S1. As expected, we found that baseline eGFR, a marker of kidney disease severity, strongly correlated with multiple histopathologic changes, such as glomerulosclerosis, RPS class, and interstitial fibrosis. Proteinuria, another key indicator of disease severity, correlated with the severity of pathological damage observed in the glomerulus, basement membrane, and tubulointerstitium. Blood pressure correlated with intimal fibrosis and body mass index with segmental sclerosis of the glomerulus.

Next, we wanted to identify the best histologic estimators for clinically relevant disease severity indicators such as kidney function (eGFR) and proteinuria (UPCR). We used multivariable linear regression analysis and included variables stepwise to identify pathologic variables that can predict the clinical changes (Table 6). We found that interstitial fibrosis showed the strongest association with eGFR at enrollment. This association remained significant and essentially unchanged after adjusting for age, gender, race, duration of DM, and HbA1C. Baseline proteinuria (UPCR) strongly correlated with glomerular parameters such as RPS class and foot process effacement.

The rate of eGFR decline (analyzed as percent eGFR change) showed the strongest association with global glomerulosclerosis and mesangiolysis, which remained significant even after adjusting for demographic and baseline eGFR. In addition, adjusting the model for clinical variables confirmed the key role of baseline eGFR in predicting eGFR decline.[35] Mesangial hyaline deposits, identified on EM were associated with UPCR change. Analyzing the time adjusted changes in eGFR or proteinuria using a mixed model approach showed similar results (data not shown).

In summary, we found significant correlations between clinical parameters and certain histopathologic changes: baseline kidney function correlated with the degree of tubulointerstitial fibrosis; eGFR change correlated with glomerular sclerosis; and albuminuria correlated with glomerular and podocyte changes.

Histology-Informed Clustering Identified 3 Disease Subgroups

Because histologic and clinical parameters showed a strong relatedness, we wanted to understand whether

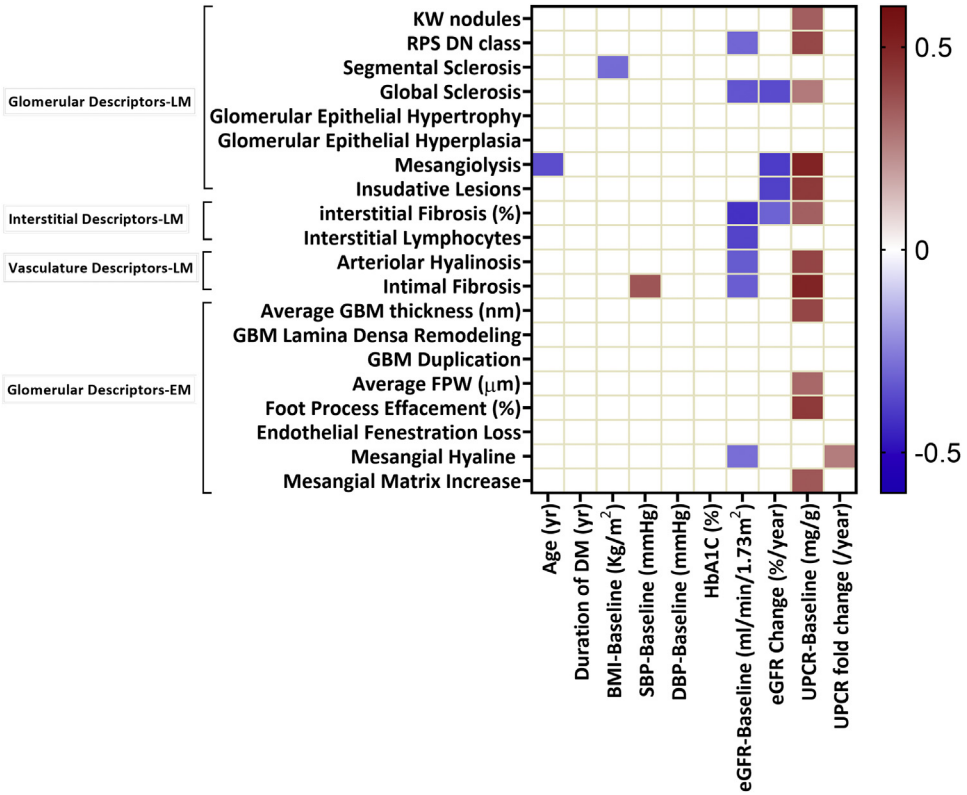

Figure 3. Correlation analysis between LM and EM descriptors and demographic and clinical parameters. Only significant correlations are shown. The color represents the strength and direction of the correlation. BMI, body mass index; DBP, diastolic blood pressure; eGFR, estimated glomerular filtration rate; EM, electron microscopy; FPW, foot process width; GBM, glomerular basement membrane; HbA1C, hemoglobin A1C; KW, Kimmelstiel-Wilson Nodule; LM, light microscopy; RPS DN class, Renal Pathology Society diabetic nephropathy class; SBP, systolic blood pressure; UPCR, urine protein to creatinine ratio.

Table 6. Multiple linear regression analysis

Dependent Variables	Adjusted R^2 (SE)	F	*P* value	Constant (SE)	*P* value	Independent Variables	Standardized B coefficient	SE	*P* value
eGFR-Baseline (ml/min per 1.73 m^2)					Unadjusted model				
	0.16 (15.45)	12.83	0.001	48.26 (4.72)	0.0001	Interstitial fibrosis (%)	−0.42	0.08	0.001
					Adjusted model[a]				
	0.16 (15.45)	12.83	0.001	48.26 (4.72)	0.0001	Interstitial fibrosis (%)	−0.42	0.08	0.001
eGFR Change (%/y)					Unadjusted model				
	0.22 (0.11)	11.25	0.001	0.33 (0.03)	0.0001	Global Sclerosis	−0.34	0.01	0.004
						Mesangiolysis	−0.31	0.03	0.009
					Adjusted model[a]				
	0.3 (0.11)	9.77	0.0001	0.44 (0.05)	0.0001	eGFR-Baseline (ml/min per 1.73 m^2)	−0.3	0.001	0.009
						Global Sclerosis	−0.44	0.01	0.0001
						Mesangiolysis	−0.33	0.03	0.003
UPCR-Baseline (mg/g)					Unadjusted model				
	0.51 (0.47)	21.68	0.0001	−1.76 (0.3)	0.0001	Intimal Fibrosis	0.51	0.08	0.0001
						Foot Process Effacement (%)	0.41	0.003	0.0001
						RPS DN Class	0.32	0.08	0.001
						Endothelial Fenestration Loss	−0.2	0.09	0.04
					Adjusted model[a]				
	0.48 (0.49)	20.15	0.0001	−1.73 (0.31)	0.0001	RPS DN Class	0.29	0.08	0.003
						Intimal Fibrosis	0.46	0.08	0.0001
						Foot Process Effacement (%)	0.36	0.003	0.0001
UPCR Fold Change (/y)					Unadjusted model				
	0.18 (0.61)	10.84	0.001	0.15 (0.16)	0.34	Mesangial Hyaline	0.42	0.07	0.001
						KW Nodules (0:NO, 1:Yes)	−0.25	0.18	0.03
					Adjusted model[a]				
	0.37 (0.54)	18.89	0.0001	0.1 (0.1)	0.32	Mesangial Hyaline	0.41	0.06	0.0001
						UPCR-Baseline (mg/g)	−0.49	0.1	0.0001

eGFR, estimated glomerular filtration rate; KW, Kimmelstiel-Wilson Nodule; RPS DN Class, Renal Pathology Society diabetic nephropathy class; SE, standard error; UPCR, urine protein to creatinine ratio.
[a]Adjusted in terms of age, gender, race, HbA1C, duration of diabetes mellitus and baseline clinical parameters (eGFR-baseline and UPCR-baseline).
All 20 pathological variables were included as independent predictors to the models; then the best fit model was calculated in a stepwise manner. In adjusted models, demographic and baseline characteristics were included in addition to pathological features.

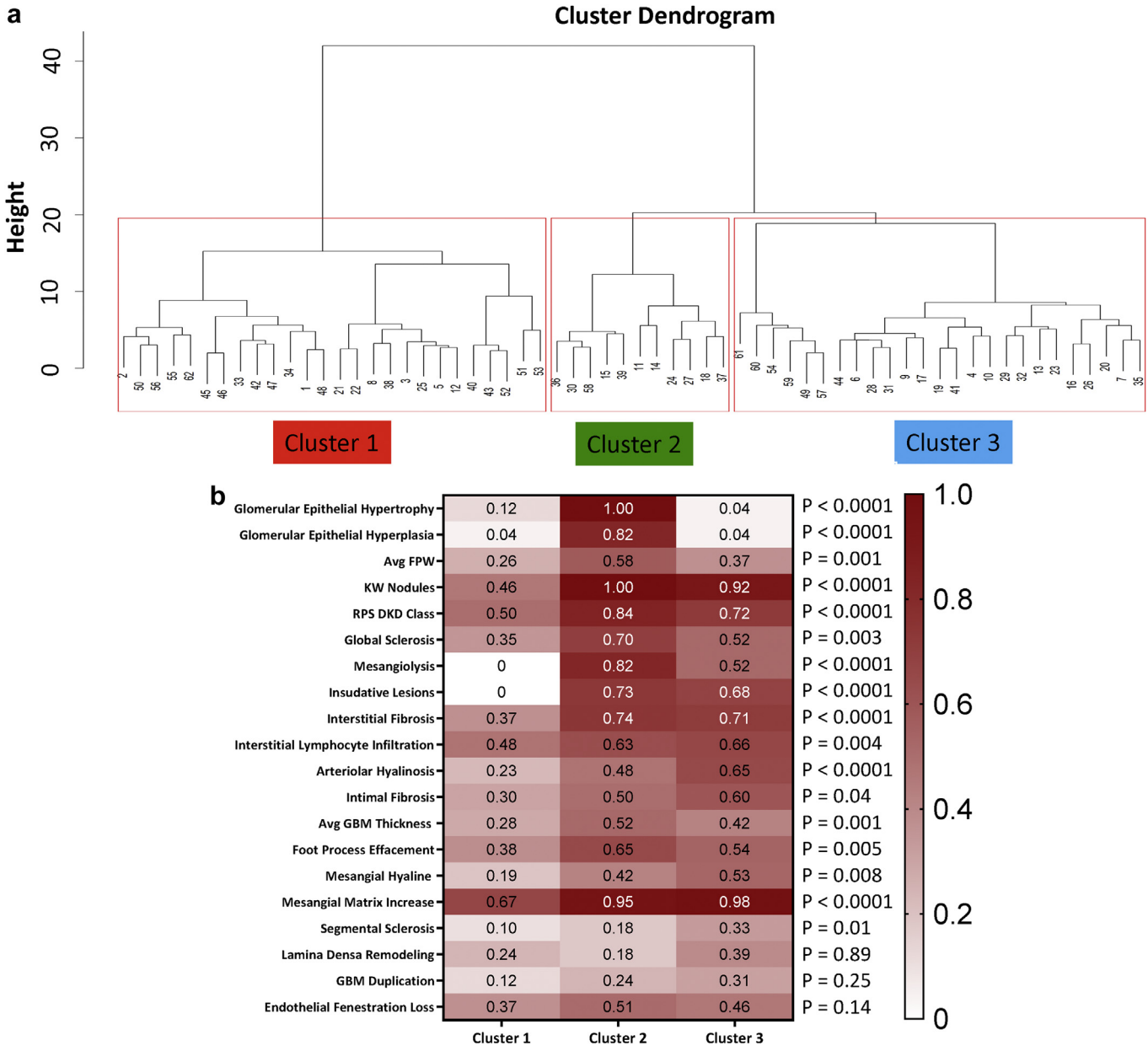

Figure 4. Histopathology-based clustering. (a) Hierarchical clustering dendrogram defines 3 distinct subgroups. (b) Heat map of scaled mean descriptors in the 3 clusters. The color indicates the scale value. Data are shown in the order of differences between clusters. Avg FPW, average foot process width; Avg GBM, average glomerular basement membrane; KW, Kimmelstiel-Wilson nodule; RPS DN class, Renal Pathology Society diabetic nephropathy class. The *P* values obtained from 1-way analysis of variance test between groups.

histologic parameters could identify disease subgroups. We performed unsupervised hierarchical clustering using only the LM and EM descriptors. The optimal number of clusters was found to be 3 (average silhouette width = 0.6). Figure 4 shows the cluster dendrogram and 3 distinct clusters.

Figure 4b depicts the mean values of each LM and EM descriptors in each cluster after scaling of the parameters (0 to 1). Cluster 1 included subjects with relatively mild changes in most histologic descriptors, indicating mostly a difference in disease severity. On the other hand, clusters 2 and 3 contained subjects with more severe LM and EM changes. Figure 5 depicts radar plots and summarizes the comparison of clinical and pathologic findings between the clusters. Indeed, clusters 2 and 3 were highly similar to each other in most parameters, and differed only in measures of epithelial cells and podocyte injury; with cluster 2 showing more severe injury.

Table 7 shows the demographic, clinical, and pathologic findings of the subjects in each cluster. As demographic and clinical parameters were not used for the clustering, we next wanted to understand whether the unbiased histopathologic grouping could provide

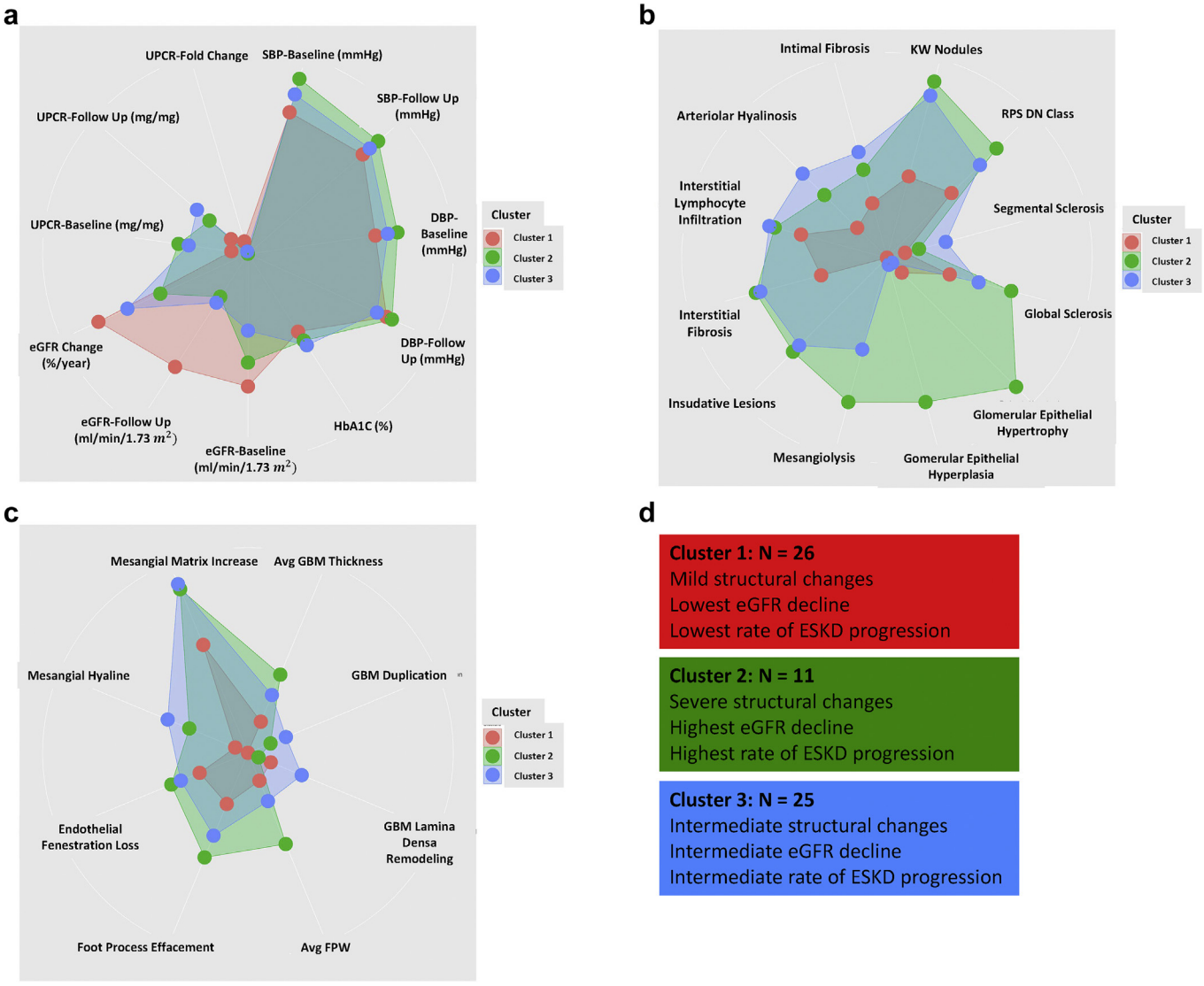

Figure 5. Radar plots of clinical, LM, and EM characteristics in different clusters. Data are shown after scaling and each dot represents one characteristic and the lengths of the spokes show the scaled magnitude of the feature. Data are arranged based on discriminative features. Each cluster is represented by a specific color (red, cluster 1; green, cluster 2; and blue, cluster 3). (a) Clinical features. (b) Light microscopic descriptors. (c) Electron microscopic descriptors. (d) Summary of differences between clusters. Avg FPW, average foot process width; Avg GBM, average glomerular basement membrane; DBP, diastolic blood pressure; eGFR, estimated glomerular filtration rate; EM, electron microscopy; HbA1c, hemoglobin A1C; KW nodules, Kimmelstiel-Wilson nodules; LM, light microscopy; RPS DN class, Renal Pathology Society diabetic nephropathy class; SBP, systolic blood pressure; UPCR, urine protein to creatinine ratio.

important information on clinical characteristics and outcome. The age, race, and gender distribution of the cases were similar in each cluster. We did not detect differences in the length of diabetes, body mass index, blood pressure, or diabetes control. On the other hand, baseline eGFR was significantly different between the clusters, with cluster 1 having the highest eGFR (39.2 [SD 17.03] ml/min per 1.73 m^2), cluster 3 had the lowest eGFR (25.84 [SD 11.84] ml/min per 1.73 m^2), and cluster 2 had intermediate eGFR (33.46 [SD 21.2] ml/min per 1.73 m^2). There was also a significant difference in the baseline proteinuria, with cluster 2 having the highest proteinuria (UPCR of 10,820 [IQR 9190] mg/g).

Overall, unbiased clustering based only on histologic descriptors was able to separate the samples into subgroups with differing clinical characteristics.

Unbiased Clustering Predicts Rate of Kidney Function Decline and ESKD

Finally, we focused on reaching ESKD and the rate of kidney function decline as the clinically most important outcome measures (Supplementary Table S2).

First, we examined RPS class as the current gold standard of DKD staging. In our study, RPS class did not correlate with the eGFR change percentage (Figure 3). We also performed Cox proportional hazard

Table 7. Comparison of clinical, LM, and EM characteristics between clusters

Variables	Cluster 1 (n = 26)	Cluster 2 (n = 11)	Cluster 3 (n = 25)	P values
Clinical characteristics				
Gender (male/female), n (%)	18(69.2)/8(30.8)	8(72.7)/3(27.3)	16(64)/9(36)	0.9
Age (y)	56.05 ± 10.77	52.36 ± 12.33	51.12 ± 14.26	0.36
Race, n (%)				0.6
White	16 (61.5)	6 (54.5)	16 (64)	
African American	7 (27)	4(36.4)	8 (32)	
Asian	3 (11.5)	1(9.1)	0	
American Indian	0	0	1 (4)	
Type of DM (I/II), n (%)	3(11.5)/23(88.5)	0/11 (100)	3(12)/22(88)	0.48
Duration of DM (y)	15.08 ± 10.8	14 ± 7.78	17.04 ± 12.83	0.71
Follow-up time (mo)	10.62 ± 5.44	10.36 ± 3.88	10.56 ± 5.27	0.99
BMI-Baseline (kg/m^2)	34.82 ± 6.6	30.89 ± 6.43	34.64 ± 8.72	0.13
BMI-Follow-up (kg/m^2)	33.84 ± 6.27	30.86 ± 6.84	35.23 ± 10.67	0.36
SBP-Baseline (mm Hg)	136.54 ± 24.26	147.73 ± 24.18	142.52 ± 18.65	0.34
SBP-Follow-up (mm Hg)	135 ± 18.4	141 ± 20.53	137.72 ± 22	0.7
DBP-Baseline (mm Hg)	74.88 ± 11.52	79.18 ± 16.73	77.28 ± 11.58	0.6
DBP-Follow-up (mm Hg)	75.54 ± 10.86	76.45 ± 12.64	73.92 ± 12.65	0.81
HbA1C (%)	7.68 ± 1.44	7.79 ± 2.13	8.1 ± 2.05	0.71
eGFR-Baseline (ml/min per 1.73 m^2)	39.2 ± 17.03	33.46 ± 21.2	25.84 ± 11.84	**0.01**
eGFR-Follow-up (ml/min per 1.73 m^2)	36.67 ± 15.11	15.27 ± 11.99	17.08 ± 7.75	**0.0001**
eGFR change (%/y)	-8.15 (35)	-72.5 (69)	-34.92 (44)	**0.005**
UPCR-Baseline (mg/g)	1340 (4130)	10820 (9190)	6250 (5600)	**0.002**
UPCR-Follow-up (mg/g)	1100 (4240)	6670 (15730)	7400 (7560)	**0.04**
UPCR fold change (/y)	1.59 (5.15)	0.99 (0.97)	1.37 (2.28)	0.54
ESKD Progression, n (%)	1 (4)	6 (54.5)	10 (38.5)	**0.002**
LM Characteristics				
KW Nodules (No/Yes), n (%)	14 (53.8)/12 (46.2)	0/11(100)	2(8)/23(92)	**0.0001**
RPS DN Class (1/2/3/4), n (%)	2(7.7)/11(42.3)/11(42.3)/2(7.7)	0/0/5(45.5)/6(54.5)	0/1(4)/19(76)/5(20)	**0.0001**
Segmental Sclerosis (0/1/2/3/4), n (%)	18(69.2)/8(30.8)/0/0/0	6(54.5)/4(36.4)/1(9.1)/0/0	5(20)/17(68)/1(4)/2(8)/0	**0.01**
Global Sclerosis (0/1/2/3/4), n (%)	2(7.7)/13(50)/9(34.6)/2(7.7)/0	0/2(18.2)/2(18.2)/3(27.2)/4(36.4)	0/7(28)/12(48)/3(12)/3(12)	**0.01**
Glomerular Epithelial Hypertrophy (0/1/2/3), n (%)	23(88.5)/3(11.5)/0/0	0/11(100)/0/0	24(96)/1(4)/0/0	**0.0001**
Glomerular Epithelial Hyperplasia (0/1/2/3), n (%)	25(96.1)/1(3.9)/0/0	2(18.2)/9(81.8)/0/0	24(96)/1(4)/0/0	**0.0001**
Mesangiolysis (No/Yes), n (%)	26(100)/0	2(18.2)/9(81.8)	12(48)/13(52)	**0.0001**
Insudative lesion (No/Yes), n (%)	26(100)/0	3(27.3)/8(72.7)	8(32)/17(68)	**0.0001**
Interstitial Fibrosis, 0–25%/25%–50%/50%–75%/75%–100%, n (%)	9 (34.6)/13 (50)/2 (7.7)/2 (7.7)	1 (9.1)/2 (18.2)/2 (18.2)/6 (54.5)	1 (4)/4 (16)/13 (52)/7 (28)	**0.0001**
Interstitial Lymphocyte (0/1/2/3), n (%)	1(3.8)/12(46.2)/13(50)/0	0/2(18.2)/8(72.7)/1(9.1)	1(4)/2(8)/18(72)/4(16)	**0.04**
Arteriolar Hyalinosis (0/1/2/3), n (%)	10(38.5)/15(57.7)/0/1(3.8)	1(9.1)/5(45.4)/4(36.4)/1(9.1)	0/7(28)/12(48)/6(24)	**0.0001**
Intimal Fibrosis (0/1/2/3), n (%)	0/12(46.1)/12(46.1)/2(7.8)	0/3(27.3)/5(45.5)/3(27.3)	0/5(20)/10(40)/10(40)	0.07
EM Characteristics				
Avg GBM thickness (nm)	690.19 ± 183.88	910.45 ± 230.16	814.56 ± 157.84	**0.003**
GBM Lamina Densa Remodeling (0/1/2/3), n (%)	13(50)/10(38.5)/0/3(11.5)	6(54.5)/4(36.4)/1(9.1)/0	8(32)/10(40)/1(4)/6(24)	0.34
GBM Duplication (0/1/2/3), n (%)	20(76.9)/4(15.4)/0/2(7.7)	5(45.5)/4(36.4)/2(18.2)/0	12(48)/7(28)/1(4)/5(20)	0.05
Avg FPW (μm)	1.51 ± 0.68	2.69 ± 1.15	1.89 ± 0.74	**0.001**
Foot process effacement (0–25%/25%–50%/50%–75%/75%–100%), n (%)	5 (19.2)/7 (26.9)/11 (42.4)/3 (11.5)	0/2 (18.2)/4 (36.4)/5 (45.5)	0/5 (20)/14 (56)/6 (24)	0.06
Endothelial fenestration loss (0/1/2/3), n (%)	4(15.4)/15(57.7)/7(26.9)/0	2(18.2)/2(18.2)/6(54.5)/1(9.1)	0/18(72)/4(16)/3(12)	**0.01**
Mesangial hyaline (0/1/2/3), n (%)	16(61.5)/7(27)/1(3.8)/2(7.7)	2(18.2)/4(36.3)/5(45.5)/0	5(20)/8(32)/4(16)/8(32)	**0.001**
Mesangial matrix increase (0/1/2/3), n (%)	0/4(15.4)/9(34.6)/13(50)	0/0/1(9.1)/10(90.9)	0/0/1(4)/24(96)	**0.002**

Avg FPW, average foot process width; Avg GBM, average glomerular basement membrane; BMI, body mass index; DBP, diastolic blood pressure; eGFR, estimated glomerular filtration rate; EM, electron microscopy; ESKD, end-stage kidney disease; KW, Kimmelstiel-Wilson Nodule; LM, light microscopy; RPS DN class, Renal Pathology Society diabetic nephropathy class; SBP, systolic blood pressure; UPCR, urine protein to creatinine ratio.

ratio as a time adjusted analysis and found that RPS class also did not predict ESKD (P values of the test in each RPS class were as follows: RPS Class 1, $P = 0.1$, RPS Class 2, $P = 0.94$; RPS Class 3, $P = 0.93$; RPS Class 4, $P = 0.92$).

By contrast, our unbiased clustering showed a significant association with eGFR change. Although kidney function was relatively stable in cluster 1, it showed a rapid decline in cluster 2. To compare the probability of reaching ESKD, among the different

subgroups we again performed Cox proportional hazard analysis and found that cluster 2 had the highest risk of ESKD progression during the follow-up time (hazard ratio: 17.89; 95% confidence interval: 2.13–149.79; $P = 0.008$) (Supplementary Table S2).

Next, we performed univariate Cox proportional hazard analysis for all available pathologic descriptors. We found that glomerular epithelial hyperplasia, GBM lamina densa remodeling, and interstitial fibrosis were predictors of ESKD progression (Supplementary Table S2). Next, we performed Kaplan-Meier analysis on the pathological variables that reached the significant threshold in univariate Cox proportional hazard analysis and compared the probability of reaching ESKD during follow-up time in different subgroups (Figure 6). We showed that patients in cluster 2 who had the most severe pathological changes, had the highest probability to ESKD at event time. Also, patients who had glomerular epithelial hyperplasia had lower renal survival rate during follow-up time (Figure 6).

Finally, we performed a multivariate Cox proportional hazard model for ESKD by including all variables that reached significance in the univariate model. We adjusted the model for clinical variables, such as age, gender, race, duration of DM, HbA1C, and baseline UPCR, based on their known association with kidney function decline. All the variables that included to the final model had reached the condition of Cox proportionality. As reported before, we found that the degree of interstitial fibrosis predicted reaching ESKD. Interestingly, glomerular epithelial hyperplasia was the strongest predictor of reaching ESKD (Table 8, Figure 7).

In summary, our analysis found that in the TRIDENT cohort, RPS class was not a strong predictor of kidney function decline or ESKD, whereas histopathologic descriptors for glomerular epithelial and podocyte injury as part of unbiased clustering or in a multivariate analysis are the strongest predictor for the rate of kidney function decline or ESKD.

DISCUSSION

Here we performed a comprehensive and unbiased descriptor-based evaluation of kidney histopathology and identified correlations with kidney functional parameters and prognosis in patients with DKD. Our analytical strategy included unbiased clustering and outcome-based analysis to identify variables that predict disease severity or prognosis. We found that different structural domains correlated with kidney function (eGFR) and prognosis (eGFR decline): while tubulointerstitial fibrosis strongly correlated with eGFR, glomerular changes showed association with eGFR decline. A strength of the study is that our cohort included samples from 11 clinical sites, representing an ethnically diverse population of the United States, in contrast to previous studies that were mostly limited to DM I or specific ethnicities, such as American Indian individuals.[26,27,36–41]

Proteinuria represents an important clinical diagnostic indicator of diabetic kidney disease. UPCR at enrollment and change correlated the best with ultrastructural estimation of podocyte foot process effacement.[42] The association between podocyte foot process effacement and proteinuria has been well documented both in animal model studies and other glomerular disease models.[43,44] In addition to podocyte foot process effacement, mesangial hyaline deposition also correlated with proteinuria,[43] as previously described by Looker *et al*.[26] The correlation between proteinuria and GBM thickness was observed in our univariate analysis; however, the observation was no longer significant after adjusting for covariates.

Interstitial fibrosis represents the terminal and common pathway to reach ESKD in patients with DKD or other causes of CKD.[45] In our study, eGFR at enrollment was independently associated with interstitial fibrosis. Several prior studies proposed that interstitial fibrosis is a predictor of CKD progression,[16,17,24,46] although most of these studies are from single centers, included samples with mixed disease etiology,[18] or were based on models that did not adjust for key variables such as baseline kidney function. Consistently with data from Mottl *et al*.[14] and Menn-Josephy *et al*.[47] in the multivariable linear regression model, fibrosis no longer predicted the slope of the eGFR decline. Overall the role of fibrosis as a prognostic marker needs further evaluation, as its correlation with outcome was relatively weak, but its association with baseline eGFR is strong and highly reproducible.

An important novelty of the work is the unbiased clustering of the samples based on histopathologic descriptors. This method was recently used in EM images from patients with nephrotic syndrome that included samples with minimal change, focal segmental glomerulosclerosis, or membranous nephropathy.[42] The method, however, has not been applied to a condition previously considered as a single disease entity, such as DKD. The 3 clusters generated based purely on histopathologic features were not different in terms of duration of DM, HbA1C, race, and age. As expected, the cluster with the least severe structural changes had the highest eGFR and the lowest eGFR decline. Clusters 2 and 3 were very similar except for differences in the degree of glomerular epithelial hypertrophy and hyperplasia.

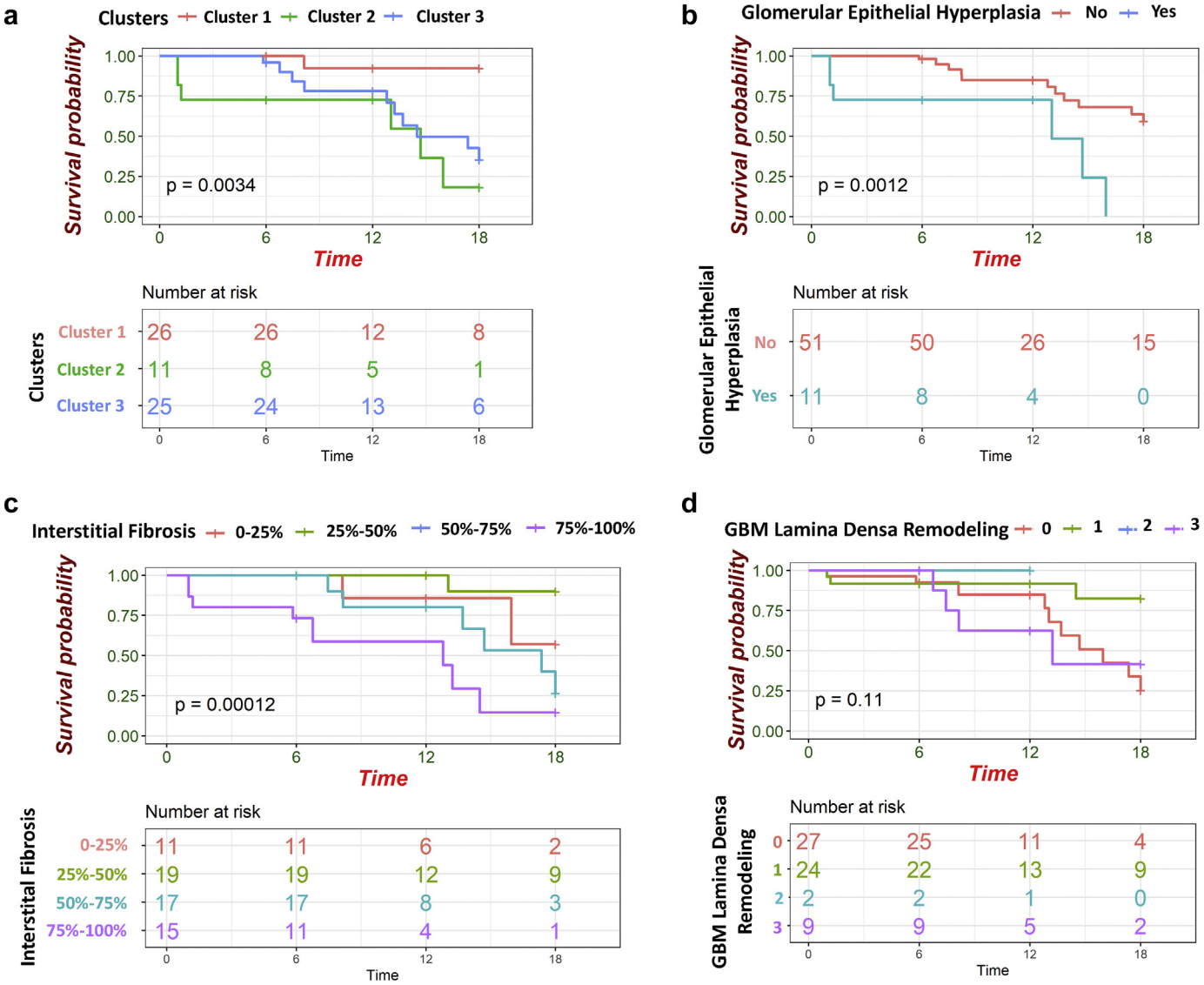

Figure 6. The Kaplan-Meier plots of parameters reach to significant threshold in Cox proportional hazard analysis. (a) Patients in cluster 2 with severe pathological changes had the lowest renal survival rate. (b) patients with glomerular epithelial hyperplasia had lower renal survival rate. (c) Higher degree of interstitial fibrosis causes lower renal survival probability. (d) Kaplan-Meier plot of glomerular basement membrane (GBM) Lamina Densa remodeling in renal survival probability. To compare the renal survival probability between sub groups Log-rank test was used. Time was considered as months from renal biopsy.

Cluster 2 with the more severe glomerular epithelial hyperplasia had the most rapid kidney function decline and the highest probability to reach ESKD. Glomerular epithelial hyperplasia appeared as the driver of the unbiased clustering analysis and showed the strongest risk for ESKD in the multivariate Cox proportional hazard model. Our findings show the potential for extracting clinically meaningful information based on pathologic features beyond the RPS classification system, and in particular, highlight the importance of changes in glomerular epithelial cells in diseases other than those traditionally considered as podocytopathies.[48]

The role of podocyte injury and adaptation in kidney function decline is consistent with prior single-center analysis showing the predictive value of segmental sclerosis predicting kidney function decline.[14] Glomerular epithelial hypertrophy and hyperplasia have been proposed as key mechanisms of disease progression in prior animal model studies.[49,50] Glomerular epithelial hypertrophy is part of an early maladaptive compensation to glomerulomegaly observed in patients with diabetes, obesity, or nephrectomy.[51,52] Podocytes are terminally differentiated cells with limited ability to proliferate.[53] Once podocytes are lost, the remaining cells must undergo

Table 8. Multivariate Cox proportional hazard analysis of pathological findings predicting ESKD after adjusting for age, race, gender, duration of DM, HbA1c, and baseline UPCR

Variables	HR	95% CI	*P* value	*P* value for the proportionality of Cox model
Glomerular epithelial hyperplasia				
0	Ref	-	-	
1	5.44	1.66–17.85	**0.005**	0.29
Interstitial fibrosis (%)				0.7
0–25	Ref	-	**0.003**	
25–50	0.33	0.02–3.92	0.38	
50–75	2.65	0.51–13.65	0.24	
75–100	9.37	1.7–51.63	**0.01**	

CI, confidence interval; DM, diabetes mellitus; ESKD, end-stage kidney disease; HbA1c, hemoglobin A1c; HR, hazard ratio; UPCR, urine protein to creatinine ratio.
The global *P* value for the Cox proportionality of the model was 0.68. The best fit model is shown.

hypertrophy to cover up the remaining surface propagating the damage. Overall, the current results together with prior publications indicate either a potential glomerular epithelial subtype of DKD or the presence of a superimposed podocytopathy in a subset of patients with DKD. Such a disease phenotype could be a particularly interesting setting in which to test the effect of podocyte-specific targeted therapeutics.

Several limitations in this study should be considered: first, the pathology scoring was performed by a single pathologist. This precludes confirmation of the reproducibility of the descriptors across multiple pathologists. To mitigate this effect, where possible we used descriptors whose definitions and reasonable reproducibility have been established in previous studies.[42,54] Second, the pathology material was collected from different sites. The absence of uniformly standardized protocols for clinical specimen preparation could contribute to potential variability in slide image presentation, quality, and EM image sampling. These issues are present in other similar multicenter studies,[42,54] and will benefit from ongoing efforts to increase standardization and automation in pathology. Third, our cohort is enriched in patients in late stages of DKD, raising the question around the generalizability of what the findings might be to patients in earlier DKD stages. As in most prior work, our study also used linear eGFR slope modeling to estimate kidney function decline. Finally, our cohort is currently of a limited sample size. As this study represents an interim analysis, we expect to further confirm and extend these studies as the TRIDENT cohort increases.

Using only clinically indicated kidney biopsy samples might appear as a limitation of the study; however, subjective biopsy criteria varied significantly in the 11 centers that participated in our study. In our study, we included only subjects with DKD in absence of any other disease-specific histopathologic lesions. Furthermore, while at present performing a kidney biopsy is not feasible for all subjects with diabetes, our study indicates that in select cases the biopsy indeed revealed important changes in glomerular epithelium and podocytes that had an observable impact on future kidney function decline. Overall, our study suggests that it might be reasonable to expand the number of biopsies performed in subjects with DKD given its important prognostic value.

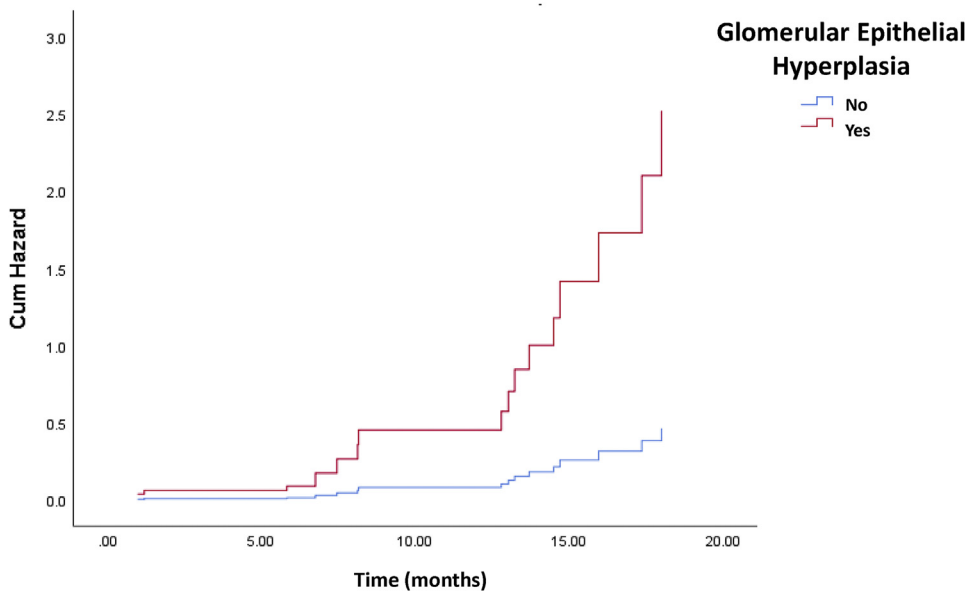

Figure 7. Cox hazard ratio plot of glomerular epithelial hyperplasia in prediction of end-stage kidney disease (ESKD). The data obtained from multivariate Cox proportional hazard ratio analysis. X-axis shows the time and y-axis represents the cumulative hazard ratio. The status of glomerular epithelial hyperplasia is shown by different colors (No glomerular epithelial hyperplasia: blue; having glomerular epithelial hyperplasia: red).

Furthermore, although our sample size might appear to be modest, given the large number of outcomes (eGFR change and ESKD) observed, we were adequately powered to detect statistically significant differences in kidney disease progression even using hard outcomes (need of renal replacement therapy). Furthermore, our study is in concordance with multiple prior studies and recent publications that analyzed a similar number of subjects.[26,55,56] As this study represents an interim analysis, we expect to further confirm and extend these studies as the TRIDENT cohort increases.

In summary, our study highlights a critical compartment-specific relationship between different clinical disease severity measurements and pathology parameters commonly reported by nephropathologists. The findings underscore the clinical relevance of histopathologic assessment of fibrosis and glomerular epithelial injury for prediction of eGFR decline in patients with diabetic nephropathy.

DISCLOSURES

KS received honoraria from Jnana and Maze Biotech, Janssen, and Chemocentryx. All the other authors declared no competing interests.

ACKNOWLEDGMENTS

The TRIDENT study is funded by Gilead, GSK, Regeneron, and Boehringer Ingelheim. The funders have no influence on the design and analysis. We thank the University of Pennsylvania Diabetes Research Center for the use of the Core (P30-DK19525). The abstract of the paper was presented in ASN kidney week 2020 as a poster and published in the abstract book.

SUPPLEMENTARY MATERIAL

Supplementary File (PDF)

Table S1. Correlation analysis between pathological parameters and clinical characteristics.

Table S2. Univariate Cox Proportional Hazard analysis of clinical and pathological findings in predicting ESKD.

REFERENCES

1. Wen CP, Chang CH, Tsai MK, et al. Diabetes with early kidney involvement may shorten life expectancy by 16 years. *Kidney Int*. 2017;92:388–396.
2. Fan W. Epidemiology in diabetes mellitus and cardiovascular disease. *Cardiovasc Endocrinol*. 2017;6:8.
3. Ameh OI, Okpechi IG, Agyemang C, et al. Global, regional, and ethnic differences in diabetic nephropathy. In: Roelofs JJ, Vogy L, eds. *Diabetic Nephropathy*. Cham, Switzerland: Springer; 2019: 33–44.
4. Brosius FC 3rd, Alpers CE, Bottinger EP, et al. Mouse models of diabetic nephropathy. *J Am Soc Nephrol*. 2009;20:2503–2512.
5. Igo RP Jr, Iyengar SK, Nicholas SB, et al. Genomewide linkage scan for diabetic renal failure and albuminuria: the FIND study. *Am J Nephrol*. 2011;33:381–389.
6. Salem RM, Todd JN, Sandholm N, et al. Genome-wide association study of diabetic kidney disease highlights biology involved in glomerular basement membrane collagen. *J Am Soc Nephrol*. 2019;30:2000–2016.
7. Gluck C, Ko Y-A, Susztak K. Precision medicine approaches to diabetic kidney disease:tissue as an issue. *Curr Diab Rep*. 2017;17:30.
8. Afkarian M, Zelnick LR, Hall YN, et al. Clinical manifestations of kidney disease among US adults with diabetes, 1988–2014. *JAMA*. 2016;316:602–610.
9. Robles NR, Villa J, Gallego RH. Non-proteinuric diabetic nephropathy. *J Clin Med*. 2015;4:1761–1773.
10. Halimi JM. The emerging concept of chronic kidney disease without clinical proteinuria in diabetic patients. *Diabetes Metab*. 2012;38:291–297.
11. Ho K, McKnight AJ. The changing landscape of diabetic kidney disease:new reflections on phenotype, classification, and disease progression to influence future investigative studies and therapeutic trials. *Adv Chronic Kidney Dis*. 2014;21:256–259.
12. Mogensen CE, Christensen CK, Vittinghus AE. The stages in diabetic renal disease. With emphasis on the stage of incipient diabetic nephropathy. *Diabetes*. 1983;2(suppl. 2):64–78.
13. Tervaert TWC, Mooyaart AL, Amann K, et al. Pathologic classification of diabetic nephropathy. *J Am Soc Nephrol*. 2010;21:556–563.
14. Mottl AK, Gasim A, Schober FP, et al. Segmental sclerosis and extracapillary hypercellularity predict diabetic ESRD. *J Am Soc Nephrol*. 2018;29:694–703.
15. Koye DN, Magliano DJ, Reid CM, et al. Risk of progression of nonalbuminuric CKD to end-stage kidney disease in people with diabetes:the CRIC (Chronic Renal Insufficiency Cohort) Study. *Am J Kidney Dis*. 2018;72:653–661.
16. Mariani LH, Martini S, Barisoni L, et al. Interstitial fibrosis scored on whole-slide digital imaging of kidney biopsies is a predictor of outcome in proteinuric glomerulopathies. *Nephrol Dial Transplant*. 2018;33:310–318.
17. Rodríguez-Iturbe B, Johnson RR, Herrera-Acosta J. Tubulointerstitial damage and progression of renal failure. *Kidney Int*. 2005;68:S82–S86.
18. Srivastava A, Palsson R, Kaze AD, et al. The prognostic value of histopathologic lesions in native kidney biopsy specimens: results from the Boston Kidney Biopsy Cohort Study. *J Am Soc Nephrol*. 2018;29:2213–2224.
19. Makino M, Yoshimoto R, Ono M, et al. Artificial intelligence predicts the progression of diabetic kidney disease using big data machine learning. *Sci Rep*. 2019;9:1–9.
20. Ninomiya T, Perkovic V, De Galan BE, et al. Albuminuria and kidney function independently predict cardiovascular and renal outcomes in diabetes. *J Am Soc Nephrol*. 2009;20:1813–1821.
21. Krolewski AS, Skupien J, Rossing P, et al. Fast renal decline to end-stage renal disease: an unrecognized feature of nephropathy in diabetes. *Kidney Int*. 2017;91:1300–1311.
22. Inker LA, Coresh J, Sang Y, et al. Filtration markers as predictors of ESRD and mortality: individual participant data meta-analysis. *Clin J Am Soc Nephrol*. 2017;12:69–78.
23. Levey AS, Gansevoort RT, Coresh J, et al. Change in albuminuria and GFR as end points for clinical trials in early stages of CKD: a scientific workshop sponsored by the

National Kidney Foundation in collaboration with the US Food and Drug Administration and European Medicines Agency. *Am J Kidney Dis*. 2020;75:84–104.

24. An Y, Xu F, Le W, et al. Renal histologic changes and the outcome in patients with diabetic nephropathy. *Nephrol Dial Transplant*. 2015;30:257–266.
25. Fufaa GD, Weil EJ, Lemley KV, et al. Structural predictors of loss of renal function in American Indians with type 2 diabetes. *Clin J Am Soc Nephrol*. 2016;11:254–261.
26. Looker HC, Mauer M, Saulnier P-J, et al. Changes in albuminuria but not GFR are associated with early changes in kidney structure in type 2 diabetes. *J Am Soc Nephrol*. 2019;30:1049–1059.
27. Pagtalunan ME, Miller PL, Jumping-Eagle S, et al. Podocyte loss and progressive glomerular injury in type II diabetes. *J Clin Invest*. 1997;99:342–348.
28. Townsend RR, Guarnieri P, Argyropoulos C, et al. Rationale and design of the Transformative Research in Diabetic Nephropathy (TRIDENT) Study. *Kidney Int*. 2020;97:10–13.
29. Levey AS, Stevens LA, Schmid CH, et al. A new equation to estimate glomerular filtration rate. *Ann Intern Med*. 2009;150:604–612.
30. Weldegiorgis M, de Zeeuw D, Li L, et al. Longitudinal estimated GFR trajectories in patients with and without type 2 diabetes and nephropathy. *Am J Kidney Dis*. 2018;71:91–101.
31. van den Bergh Weerman MA, Assmann KJ, Weening JJ, et al. Podocyte foot process effacement is not correlated with the level of proteinuria in human glomerulopathies. *Kidney Int*. 2004;66:1901–1906.
32. Haas M. Alport syndrome and thin glomerular basement membrane nephropathy: a practical approach to diagnosis. *Arch Pathol Lab Med*. 2009;133:224–232.
33. Kimes PK, Liu Y, Neil Hayes D, et al. Statistical significance for hierarchical clustering. *Biometrics*. 2017;73:811–821.
34. Lengyel A, Botta-Dukát Z. Silhouette width using generalized mean—A flexible method for assessing clustering efficiency. *Ecol Evol*. 2019;9:13231–13243.
35. Tangri N, Stevens LA, Griffith J, et al. A predictive model for progression of chronic kidney disease to kidney failure. *JAMA*. 2011;305:1553–1559.
36. Drummond K, Mauer M. The early natural history of nephropathy in type 1 diabetes: II. Early renal structural changes in type 1 diabetes. *Diabetes*. 2002;51:1580–1587.
37. Fioretto P, Steffes MW, Sutherland DE, et al. Sequential renal biopsies in insulin-dependent diabetic patients:structural factors associated with clinical progression. *Kidney Int*. 1995;48:1929–1935.
38. Fu H, Liu S, Bastacky SI, et al. Diabetic kidney diseases revisited: a new perspective for a new era. *Mol Metab*. 2019;30:250–263.
39. Mauer M, Caramori ML, Fioretto P, et al. Glomerular structural–functional relationship models of diabetic nephropathy are robust in type 1 diabetic patients. *Nephrol Dial Transplant*. 2015;30:918–923.
40. Mauer M, Zinman B, Gardiner R, et al. Renal and retinal effects of enalapril and losartan in type 1 diabetes. *N Engl J Med*. 2009;361:40–51.
41. Mauer SM, Steffes MW, Ellis EN, et al. Structural-functional relationships in diabetic nephropathy. *J Clin Invest*. 1984;74:1143–1155.
42. Royal V, Zee J, Liu Q, et al. Ultrastructural characterization of proteinuric patients predicts clinical outcomes. *J Am Soc Nephrol*. 2020;31:841–854.
43. Jefferson J, Shankland S, Pichler R. Proteinuria in diabetic kidney disease: a mechanistic viewpoint. *Kidney Int*. 2008;74:22–36.
44. Lin JS, Susztak K. Podocytes: the weakest link in diabetic kidney disease? *Curr Diab Rep*. 2016;16:45.
45. Breyer MD, Susztak K. The next generation of therapeutics for chronic kidney disease. *Nat Rev Drug Discov*. 2016;15:568.
46. Takaori K, Nakamura J, Yamamoto S, et al. Severity and frequency of proximal tubule injury determines renal prognosis. *J Am Soc Nephrol*. 2016;27:2393–2406.
47. Menn-Josephy H, Lee CS, Nolin A, et al. Renal interstitial fibrosis:an imperfect predictor of kidney disease progression in some patient cohorts. *Am J Nephrol*. 2016;44:289–299.
48. Trimarchi H, Coppo R. Podocytopathy in the mesangial proliferative immunoglobulin A nephropathy: new insights into the mechanisms of damage and progression. *Nephrol Dial Transplant*. 2019;34:1280–1285.
49. Herbach N, Schairer I, Blutke A, et al. Diabetic kidney lesions of GIPRdn transgenic mice:podocyte hypertrophy and thickening of the GBM precede glomerular hypertrophy and glomerulosclerosis. *Am J Physiol Renal Physiol*. 2009;296:F819–F829.
50. Puelles VG, Van Der Wolde JW, Wanner N, et al. mTOR-mediated podocyte hypertrophy regulates glomerular integrity in mice and humans. *JCI Insight*. 2019;4, e99271.
51. D'Agati VD, Chagnac A, De Vries AP, et al. Obesity-related glomerulopathy:clinical and pathologic characteristics and pathogenesis. *Nat Rev Nephrol*. 2016;12:453.
52. Hommos MS, Glassock RJ, Rule AD. Structural and functional changes in human kidneys with healthy aging. *J Am Soc Nephrol*. 2017;28:2838–2844.
53. Sweetwyne MT, Gruenwald A, Niranjan T, et al. Notch1 and Notch2 in podocytes play differential roles during diabetic nephropathy development. *Diabetes*. 2015;64:4099–4111.
54. Zee J, Hodgin JB, Mariani LH, et al. Reproducibility and feasibility of strategies for morphologic assessment of renal biopsies using the nephrotic syndrome study network digital pathology scoring system. *Arch Pathol Lab Med*. 2018;142:613–625.
55. Lemley KV, Blouch K, Abdullah I, et al. Glomerular permselectivity at the onset of nephropathy in type 2 diabetes mellitus. *J Am Soc Nephrol*. 2000;11:2095–2105.
56. White KE, Bilous RW. Type 2 diabetic patients with nephropathy show structural-functional relationships that are similar to type 1 disease. *J Am Soc Nephrol*. 2000;11:1667–1673.
57. Barisoni L, Troost JP, Nast C, et al. Reproducibility of the NEPTUNE descriptor-based scoring system on whole-slide images and histologic and ultrastructural digital images. *Mod Pathol*. 2016;29:671–684.
58. Stout LC, Kumar S, Whorton EB. Insudative lesions—their pathogenesis and association with glomerular obsolescence in diabetes:a dynamic hypothesis based on single views of advancing human diabetic nephropathy. *Hum Pathol*. 1994;25:1213–1227.